Evaluation of a CMOS Imager as Readout for Imaging Photon Counters

S N Tandon, IUCAA, Ganeshkhind, Pune 411 007, India

Abstract: This work is motivated by a desire to check if CMOS detectors, which are somewhat inferior to CCDs in terms of noise and dark current, but are much simpler to use, could be used as readout in imaging photon counters. Tests have been made on the performance of a CMOS detector used as readout of an image intensifier. The main conclusions are that: a) the detector has adequate dynamic range as well as sensitivity for photon counting, b) with an optics for reduction by a factor about three between the intensifier and the readout, it is found that 10-20 micron wide slits are recorded with an rms width of ~ 0.14 pixels, i.e. ~ 11 microns on the slit-plane – this includes effects due to finite resolution of the intensifier, and c) the detector is capable of giving a rms precision of ~ 0.03 pixels (~ 0.7 microns) on centroids of images similar to those of intensified photon events.

1. Introduction

Solid state imagers provide a very convenient means of readout for imaging photon counting detectors, and CCDs and CIDs have been used extensively for this purpose (Read et al 1988, Vallerga et al 1995, P Bergamini et al 2000, Kimble et al 1995, O H W Siegmund 1999). In such detectors a photon leads to a bright spot with FWHM of 1-2 pixels on the CCD/CID, and position of the spot is estimated by finding its centroid to sub-pixel accuracy. In order to find the centroid, simple algorithms are used for real time implementation, e.g. a 3 X 3 pixel window around the brightest pixel is used and the intensity is assumed to be uniform over the face of each pixel, i.e. if the brightest pixel has a signal 'b' and its two neighbours have signals 'a' and 'c', the centroid is defined as (-a+c)/(a+b+c). While any errors due to read noise and dark noise are not significant, due to the large multiplications provided by the intensifier, systematic errors due to windowing and digitisation are significant (Fordham and Hook 1988), and it has been shown that these errors can be corrected to better than 0.1 pixel (Carter et al 1990, Bellis et al 1991).

In recent times, good CMOS imagers have become commercially available, and provide attractive alternative to CCDs in those applications where a large dynamic range is not required. In the readout of imaging photon counting detectors a large dynamic range is not required and hence CMOS detectors provide a very convenient

substitute for CCDs. However, as the pixels of CMOS detectors have much more complex structure as compared to a CCDs, it is not obvious that the systematic errors in centroiding for these can be reduced to the same level as for CCDs. For example, while CCDs seem to show systematic errors in each coordinate (x or y) which only depends on the fractional value of the coordinate in a pixel, the complex two dimensional structure of the pixels in CMOS imagers could lead to errors which are a function of both the coordinates. Therefore, it is of interest to make direct checks on the limitations of CMOS imagers for the readout. In this work we present results of tests made with Star 250 CMOS imager made by Fillfactory. In Section 2 the test set up is described, in Section 3 the method of analysis is described, and the results of tests are presented in Section 4. Conclusions are stated in Section 5.

2. Test set up

An image intensifier made by Proxitronics, with a three stage MCP multiplier and with fibre optic windows at the input as well as at the output, is used in combination with the CMOS detector. The output window of the intensifier is imaged on the CMOS detector by a set of camera lenses (see Fig. 1); this detector has 512 X 512 pixels, each of 25 X 25 microns, and is integrated in a test kit supplied by the manufacturer. Most of the images are taken with a photo-mask, having a set of 10-20 micron wide slits on a pitch of 0.5 mm, placed in contact with the input window; two sets of camera lenses are used at the output to get reductions of ~ 1:1 and ~ 1:3 respectively.

In the above tests the errors depend on the intensifier as well as on the CMOS detector. Therefore, in order to study limitations of the CMOS detector, tests are also made with images projected directly on it; a square grid of pin holes is imaged such that image of each hole has a FWHM of 1-2 pixels, i.e. Very similar to that of th photon events obtained with the intensifier. Light from a red LED has been used for all the tests.

3. Analysis of the images

3.1 Point spread function and location of the photon events

The photon events have a FWHM of ~ 70 microns at the output window of the intensifier, i.e. ~ 3 pixels on the CMOS detector when imaged with unity magnification, and ~ 1 pixel when imaged with a demagnification of 3. As the MCPs in the intensifier have pores on a pitch of ~ 12 microns, the PSF is not expected to have a large variation from event to event. Location of the photon events at the output window is expected to have a rms spread of ~ 10 microns due to: a) finite diameter of the fibres in the input window, b) transverse motion of the photo-electrons between the photo-cathode and the MCP, and c) finite size of pores in the MCPs; of the three causes "b)" is the most significant and it is larger for light of shorter wavelengths. A robust measure of location of an event is provided by coordinates of its centroid.

3.2 Finding coordinates of the centroids

The centroid of a photon event is taken as centroid of the signals in a square window; the window is centred on the brightest pixel and its size is chosen as 5 pixels for 1:1 images, and it is chosen as 3 pixels for images with reduction 1:3. As the signal is quite large any errors in the centroid coordinates due to noise are very small. However, systematic errors due to finite size of the window and digitisation are significant; we call these errors as bias and discuss their correction in the next subsection.

3.3 Finding bias in coordinates of the centroids

It is easily seen that, for a symmetrical PSF, expectation values of the coordinates calculated on a window with odd size (3 or 5 pixels) coincide with the true values, if the centroid falls on centre of a pixel. On the other hand, if the centroid falls near edge of a pixel, the calculated coordinates can have large biases (> 0.05 pixel) which depend on the PSF as well as size of the window; for a window of size 3 pixels, a PSF with a rms spread of ~ 0.5 pixels is optimal for minimising the bias.

In order to make an estimate of the bias, images are taken with uniform illumination on input window of the intensifier, and a statistical analysis of the coordinates of the photon events is made as follows: a) the coordinates are rewritten modulo one, b) pixel is divided into a grid of twenty equal columns (rows), and the number of centroids falling in each of these twenty columns (rows) is tabulated, and c) the boundaries of the columns (rows) are adjusted to give a uniform distribution of the events in all the columns (rows). The shift between the new boundaries and the old boundaries is a measure of the bias for the particular column (row). It is to be noted that this procedure is based on the assumptions that: i) the true distribution of the coordinates is uniform over each pixel, ii) any variations in PSF over face of the detector is insignificant, and iii) bias in coordinate X (Y) is independent of Y (X).

4 Results

4.1 Images without reduction

A set of 200 images is taken with a photo mask, having 10-20 micron wide slits on 0.5 mm spacing, kept in contact with the input fibre window. The illumination is adjusted to ensure that the probability of two photon events overlapping is small; an average of ~ 40 events is recorded per frame in an area of ~ 200 X 200 pixels. A window of 5 X 5 pixels centred on the brightest pixel is used to find centroids of all the photon event in each frame. The centroids obtained thus in all the frames are put together to get the final image. Part of the final image is shown in Fig. 2; the original image, in which the slits are placed at an angle of ~ 6.5 deg. to the rows, has been rotated to align the slits parallel to the ordinate. The effects of bias are clearly seen as a structure in the image of each slit. For comparison, the same part of the image is shown in Fig. 3 after applying corrections for the bias, and it can be seen that the structure within the slits has disappeared. In order to get a measure of the rms

width of the images, image of each slit is fitted to a second order polynomial and rms deviation of the events from the fit is calculated. The values of rms deviation for Fig. 2 and Fig. 3 are 0.380 (+- 0.02) pixels and 0.368 (+- 0.02) pixels respectively; thus while the errors due to the bias can be up to 0.1 pixels, their effect on the rms width is not expected to be significant. It can also be seen that these results give ~ 9.5 (9.2) microns for the rms width of the images, a value consistent with what is expected if the centroiding errors on the CMOS detector are negligible.

4.2 Images with a reduction factor 3

Another similar set of 200 images is taken with a reduction of 1:3; the frames are analysed in a fashion similar to that described above, but with a window of 3 X 3 pixels for centroiding. Part of the image obtained after digital integration of all the frames is shown in Fig. 4, and the same part of the image is shown in Fig. 5 after applying corrections for the bias. The values of rms deviations from the fits for Fig. 4 and Fig. 5 are 0.143 (+- 0.01) pixels and 0.139 (+- 0.01) pixels respectively; thus while the errors due to the bias can be up to 0.1 pixels, their effect on the rms deviations is not expected to be significant. It can also be seen that these results give ~ 10.7 (10.4) microns for the rms width of the images.

4.3 Errors in centroiding

The estimated values of the rms deviations mentioned above are a combined effect of several contributions: finite width of the slits, errors in translation from the input window to the output window of the intensifier, and errors in centroiding on the CMOS detector. The contributions of the first two errors are not expected to depend on the gain used to image the output window on the detector, whereas the contribution of the last error (normalised to the scale of the input window) is expected to be in inverse proportion of the gain. A comparison of the rms widths of the images without reduction and images with reduction, shows that the centroiding error on the imager is 0.05 to 0.1 pixels.

It is not possible to explain such a large error in centroiding in terms of the read noise and electron-count statistics in the pixels, and one should look else where for sources of this error. The sources could be either internal to the imager or external to it. In the next subsection we discuss results of the tests conducted to estimate the errors internal to the CMOS detector.

4.4 Direct imaging on the CMOS detector

The above estimate suggests that the errors in centroiding are larger than what is expected from sources of noise in the imager. Some of the possible causes for larger errors are: a) variations in the PSF of photon events and the consequent variations in the bias, and b) a dependence of bias in X (Y) on Y (X), or some other limitation due to structure of the pixels in the COMS detector. In order to make an estimate of the limitations imposed by "b)" on precision in centroiding, a mask with a line of equally spaced pin holes is directly imaged, with a reduction factor of ~ 80. Image of the line is aligned with rows (columns) of the imager, and spacing of the holes is

adjusted such that if an image of a hole falls at "N+y" pixels, image of the next hole falls at "N+y-0.1" pixels; this ensures that: a) all the images have the same X-coordinate, and b) the Y-coordinates are distributed along different locations in the pixels, so that any effect of Y on the bias in X can be seen. The mask is moved in small steps, ~ 0.12 pixels, along the columns (rows) to cover a range of one full pixel in ~ 10 images (see Fig. 6); care is taken to ensure that the signal and PSF of the images of individual holes are similar to those of the photon events recorded with the intensifier. All the images are analysed to find centroids in 3 X 3 pixel windows, and the centroids are fitted to straight lines parallel to rows (columns). The rms deviations found in the fits are ~ 0.013 (0.017) pixels, and this shows that the CMOS detector is capable of giving a rms precision of <~ 0.02 pixels on each coordinate in centroiding with a 3 X 3 window.

5 Conclusion

a) The tests carried out on the CMOS imager Star 250 with an image intensifier show that this combination can be used to get an overall rms error < 11 microns on each coordinate of individual photon events; this result is obtained with red light and the error could be larger for blue light, because of a larger error contributed by the intensifier.

b) A comparison of the images taken with 1:1 gain and the images taken with 1:3 reduction (between the output window of the intensifier and the CMOS imager) shows that contribution of the imager to the rms error is <~ 7 microns for 1:3 reduction.

c) Direct imaging with the CMOS detector shows that its contribution to the error could be < 0.5 micron on each coordinate (0.5 micron would translate to 1.5 microns on the input if a 1:3 reduction is used); while this is not inconsistent with "b)" above, this small error suggests that additional errors may be arising due to some variation in the profile of individual intensified photon events, either random or related to position in the field.

Acknowledgments:
The hardware and software for recording images with Star 250 detector at a fast rate, were developed by Mahesh Burse, Pravin Chordia, Ramaprakash, and Sunu Engineer. Abhay Kohok has taken a lot of trouble to record and analyse thousands of images with great patience. Enthusiastic help of all these colleagues from IUCAA is gratefully acknowledged.

References:

J G Bellis, D A Bone, and J L A Fordham,
PASP 103, 253 (1991)

M K Carter, R Cutler, B E Patchett, P D Read, N Waltham, and I G van Breda,
SPIE Proceedings 1235, 644 (1990)

J L A Fordham and R N Hook
Instrumentation for Ground-Based Optical Astronomy (Ed. L B Robinson),
Springer-VERLAG, 582 (1988).

R Kimble, P Chen, J P Haas, T Norton, L Payne, J Carbone, and M Corba,
SPIE Proceedings 2518, 397 (1995)

P D Read, I G Van Breda, T J Norton, R W Airey, B L Morgan, and J R Powell,
Instrumentation for Ground-Based Optical Astronomy (Ed. L B Robinson),
Springer-VERLAG, 528 (1988).

O H W Siegmund,
ASP Conference Series 164 , 374 (1999)

J Vallerga, P Jelinsky, and O Siegmund,
SPIE Proceedings 2518, 410 (1995)

Captions for the figures:

Fig. 1: The test set up is shown. The slit mask is placed in contact with the input (fibre) window of the intensifier, and the output window (phosphor) is imaged by a set of two camera lenses on the CMOS imager; the lenses either give a 1:1 image or a 1:3 reduced image.

Fig. 2: Image of the slit-mask is shown, with 1:1 gain between output window of the amplifier and the CMOS imager. The rms width of each slit-image is ~ 0.38 pixels, i.e. ~ 9.5 microns.

Fig. 3: Image of the slit-mask is shown, with 1:1 gain between output window of the amplifier and the CMOS imager, after removal of the bias (see text). The rms width of each slit-image is ~ 0.37 pixels, i.e. ~ 9.2 microns.

Fig. 4: Image of the slit-mask is shown, with 1:3 reduction between output window of the amplifier and the CMOS imager. The rms width of each slit-image is ~ 0.143 pixels, i.e. ~ 10.7 microns on the object plane.

Fig. 5: Image of the slit-mask is shown, with 1:3 reduction between output window of the amplifier and the CMOS imager, after removal of the bias (see text). The rms width of each slit-image is ~ 0.138 pixels, i.e. ~ 10.4 microns on the object plane.

Fig. 6: A set of 11 images of a line of pin holes, taken directly with the CMOS detector, is shown. Each new image is taken after shifting the line by a fixed interval along X-axis. The image on extreme left is split into two lines because of the bias which shifts the coordinates towards centres of the pixels, i.e. the points with coordinates just below "0.5" are shifted nearer to "0.4" and those with coordinate just above "0.5" are shifted closer to "0.6".

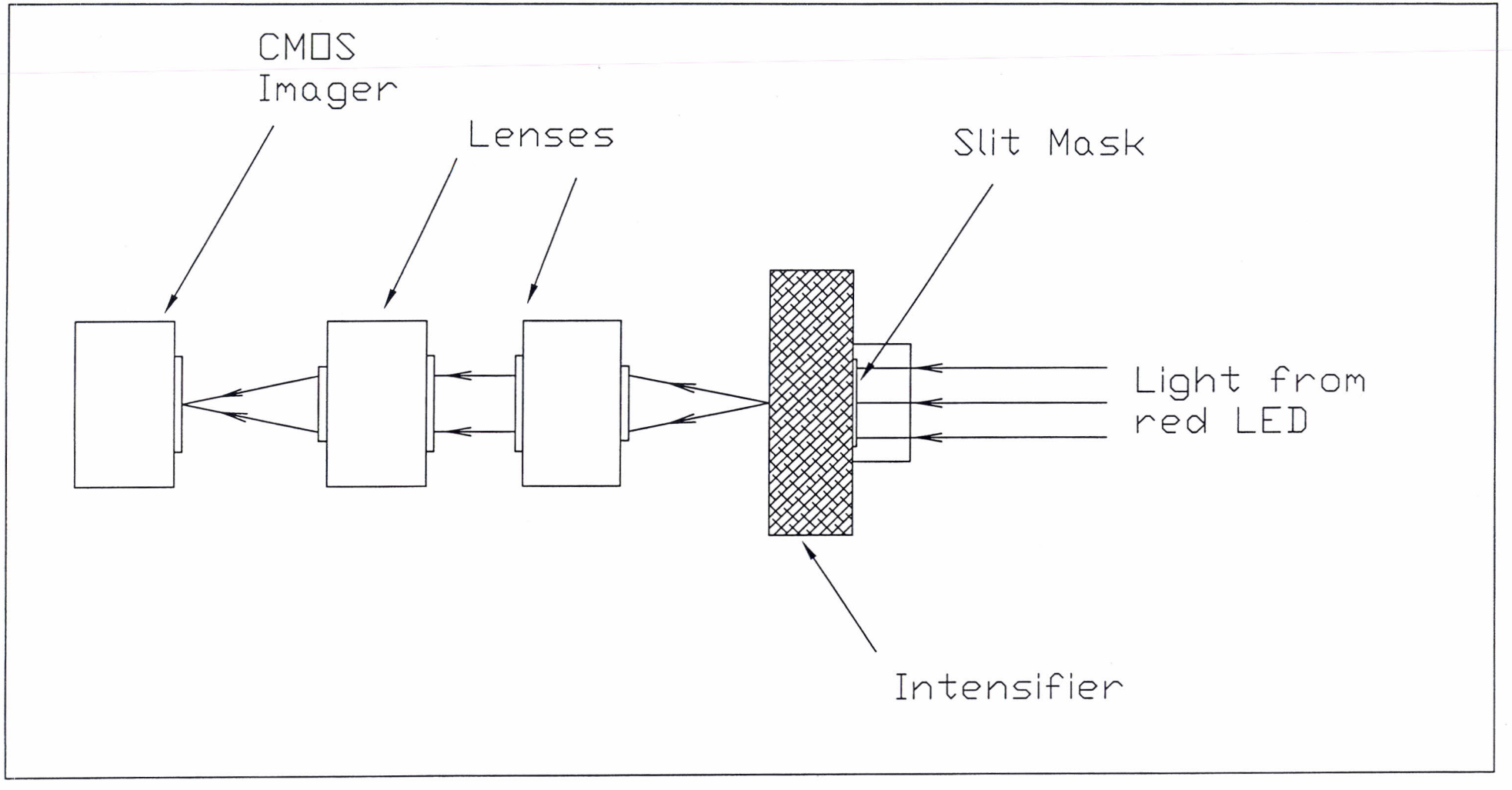

Fig. 1: The test set up is shown. The slit mask is placed in contact with the input (fibre) window of the intensifier, and the output window (phosphor) is imaged by a set of two camera lenses on the CMOS imager; the lenses either give a 1:1 image or a 1:3 reduced image.

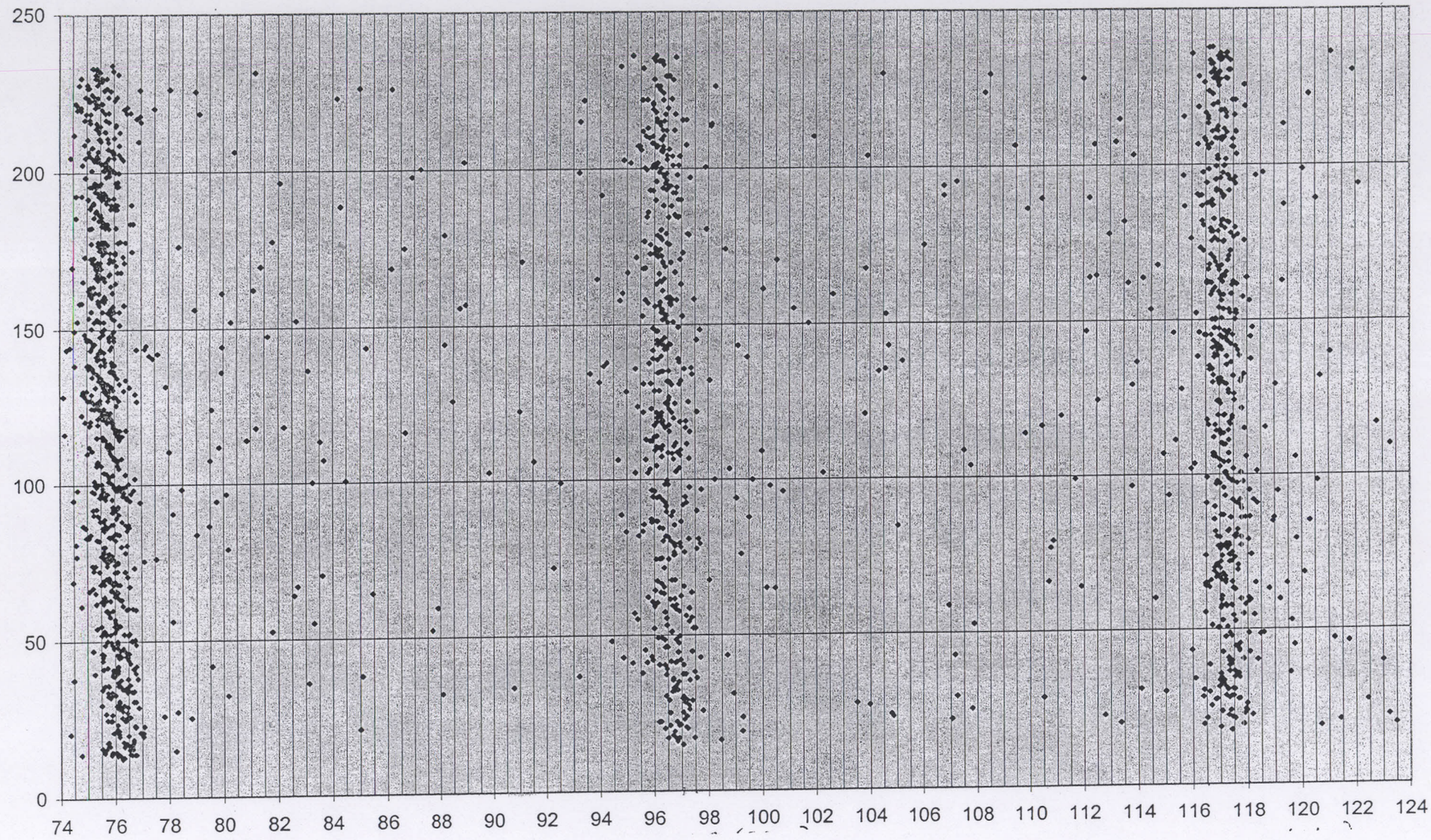

Fig. 2: Image of the slit-mask is shown, with 1:1 gain between output window of the amplifier and the CMOS imager. The rms width of each slit-image is ~ 0.38 pixels, i.e. ~ 9.5 microns.

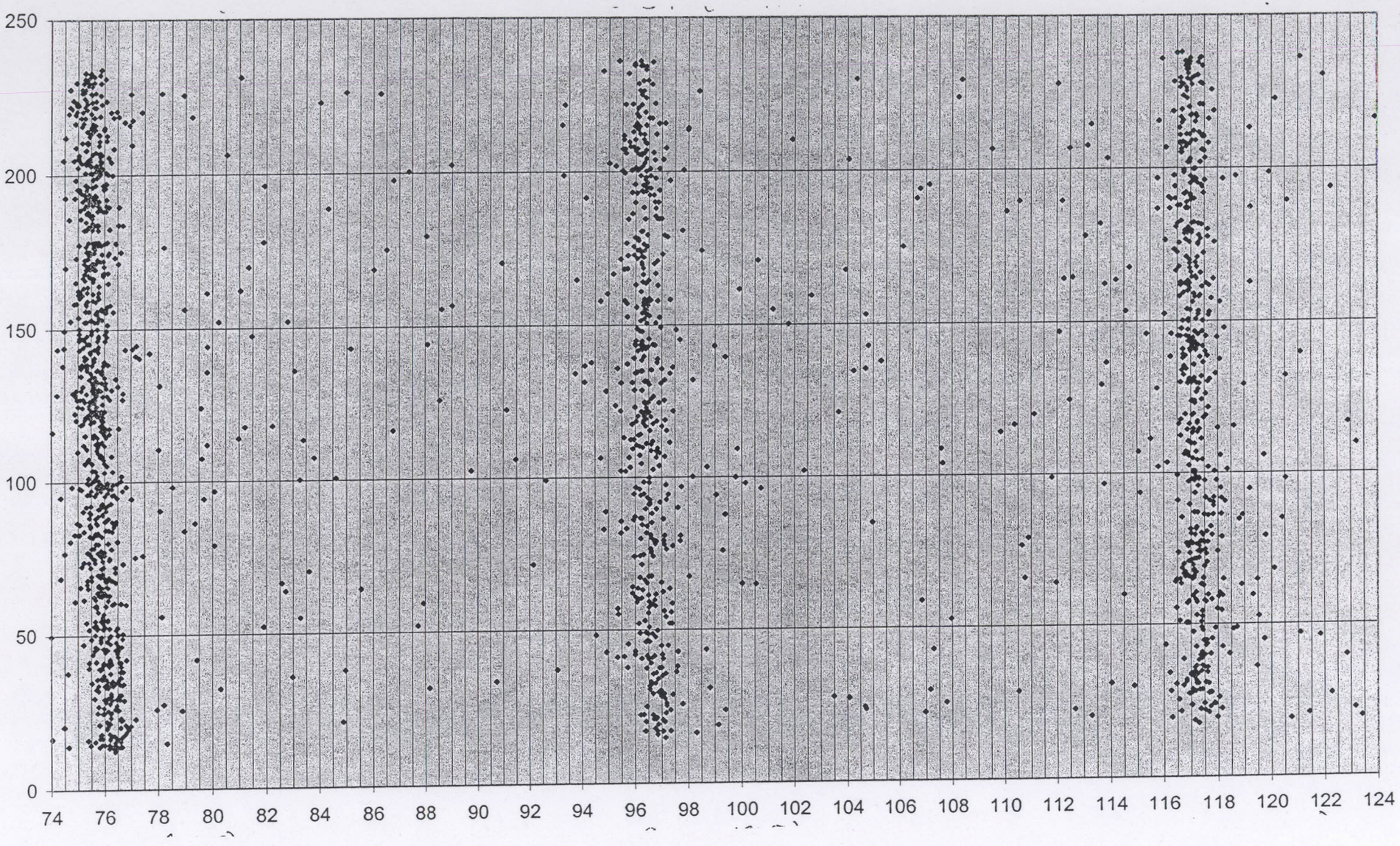

Fig. 3: Image of the slit-mask is shown, with 1:1 gain between output window of the amplifier and the CMOS imager, after tremoval of the bias (see text). The rms width of each slit-image is ~ 0.37 pixels, i.e. ~ 9.2 microns.

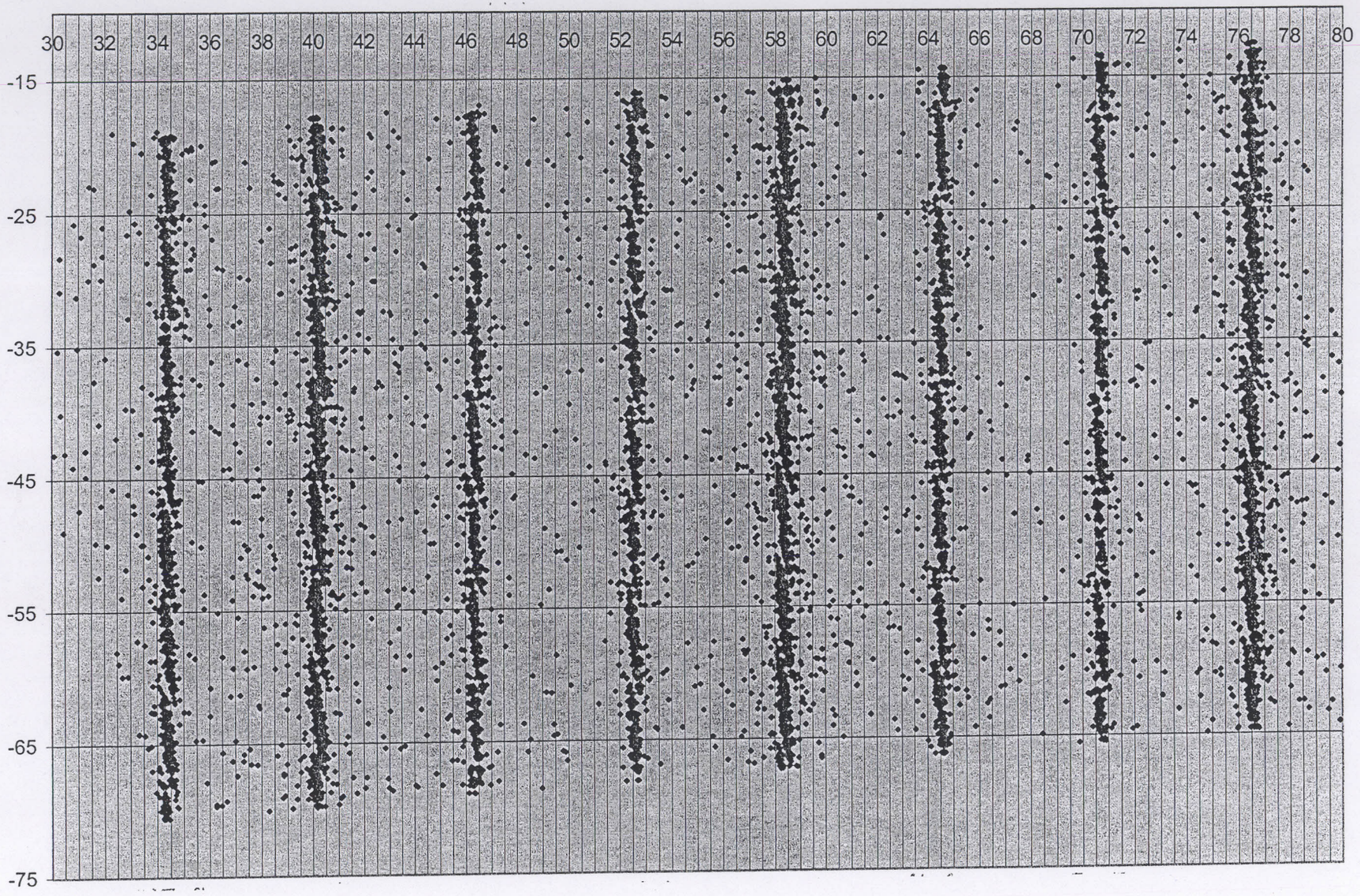

Fig. 4: Image of the slit-mask is shown, with 1:3 reduction between output window of the amplifier and the CMOS imager. The rms width of each slit-image is ~ 0.143 pixels, i.e. ~ 10.7 microns on the object plane.

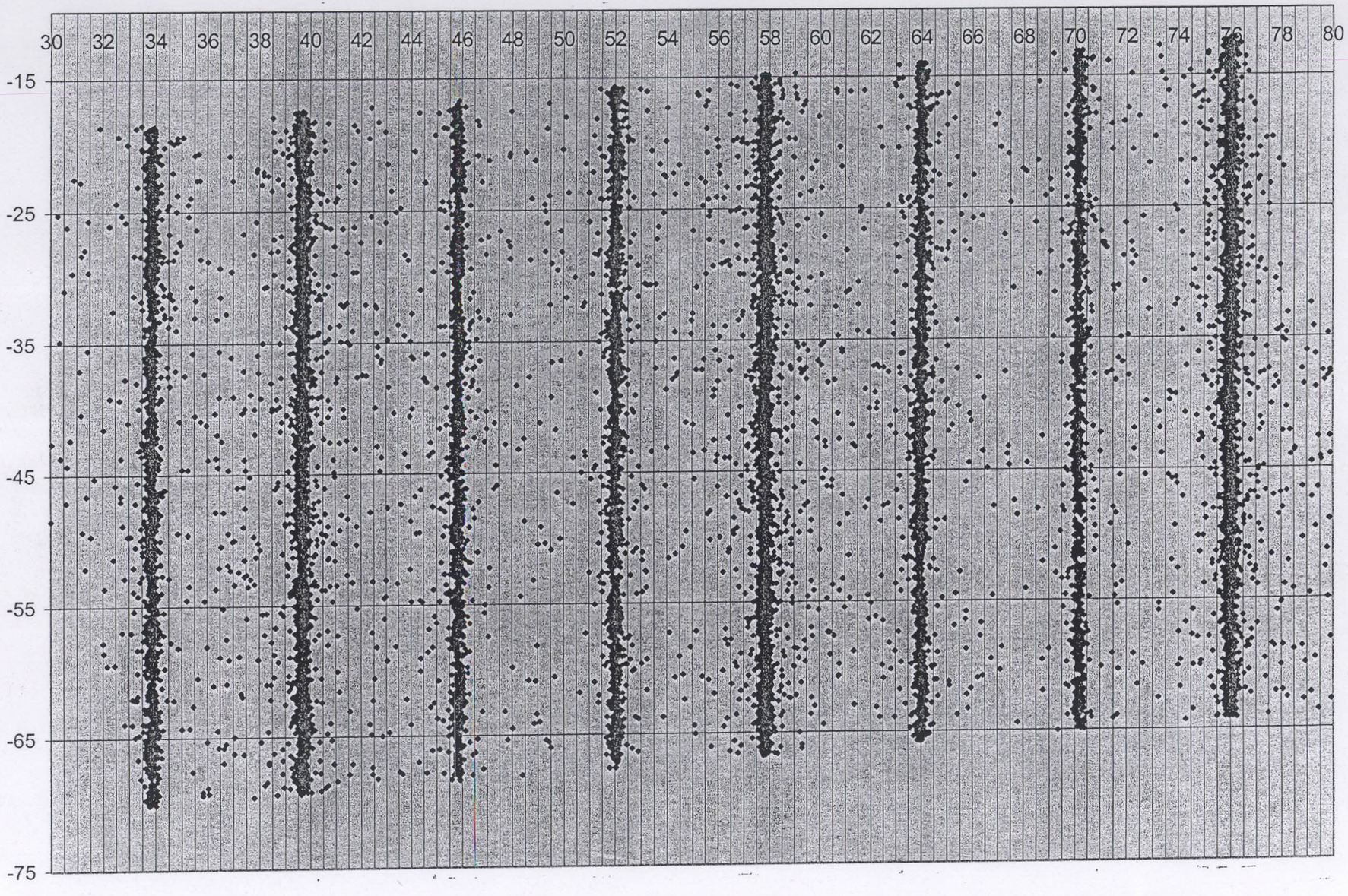

Fig. 5: Image of the slit-mask is shown, with 1:3 reduction between output window of the amplifier and the CMOS imager, after removal of the bias (see text). The rms width of each slit-image is ~ 0.138 pixels, i.e. ~ 10.4 microns on the object plane.

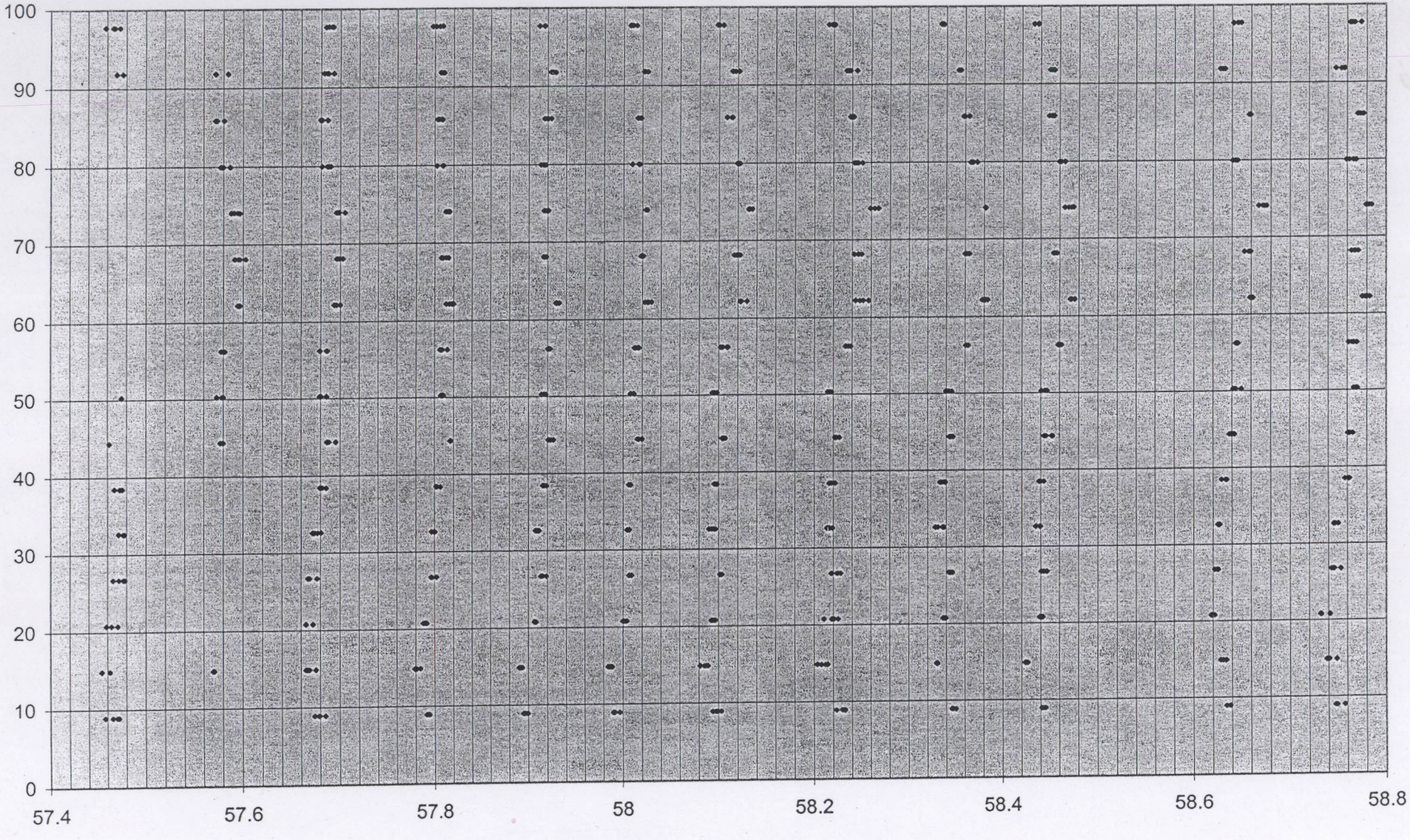

Fig. 6: A set of 11 images of a line of pin holes, taken directly with the CMOS detector, is shown. Each new image is taken after shifting the line by a fixed interval along X-axis. The image on extreme left is split into two lines because of the bias which shifts the coordinates towards centres of the pixels, i.e. the points with coordinates just below "0.5" are shifted nearer to "0.4" and those with coordinate just above "0.5" are shifted closer to "0.6".